Simulated regional dust cycle in the Carpathian Basin and the Adriatic Sea region during the Last Glacial Maximum

Patrick Ludwig[1], Milivoj B. Gavrilov[2], Slobodan B. Markovic[2], Gabor Ujvari[3], Frank Lehmkuhl[4]

[1]Institute for Meteorology and Climate Research (IMK-TRO), Karlsruhe Institute of Technology, Germany,
[2]Chair of Physical Geography, Faculty of Science, University of Novi Sad, Novi Sad, Serbia
[3]Institute for Geological and Geochemical Research, Research Centre for Astronomy and Earth Sciences, Budapest, Hungary
[4]Department of Geography, RWTH Aachen University, Aachen, Germany.

This work has been published in *Quaternary International:*

https://doi.org/10.1016/j.quaint.2020.09.048

unless otherwise stated, Figures are from this publication

Overview

Aim: Study aspects of the regional dust cycle in the Carpathian Basin and Po plain/Adriatic shelf

Methods: Study aspects of the regional dust cycle in the Carpathian Basin and Po plain/Adriatic shelf

Results: Different wind patterns responsible for dust emission / transport. Dinaric Alps act as natural barrier for dust fluxes between Carpathian Basin / Po plain & Adriatic shelf

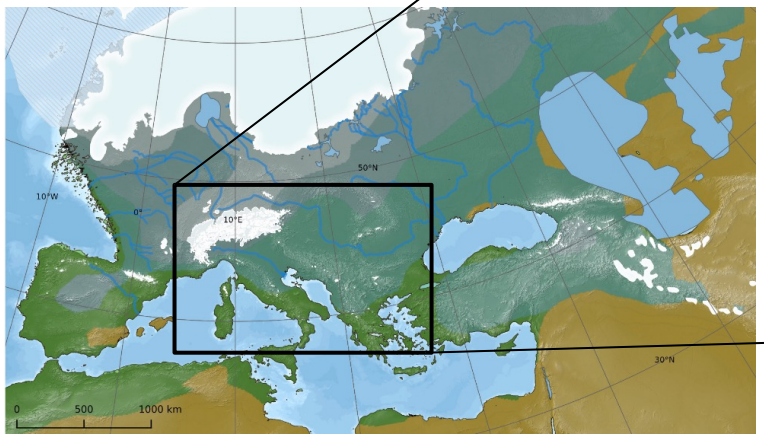
Let's get started…

https://doi.org/10.1016/j.quaint.2020.09.048

Questions

- What was the regional glacial dust cycle during the Last Glacial Maximum (LGM) in the Carpathian Basin and Adriatic Shelf region?
- What were the important climate parameters determining the dust cycle?
- Was there any dust transport across the Dinaric Alps between the two regions?

Map of glacial Europe (LGM) with zoom on study area





Maps from sfb806.de; doi:10.5880/SFB806.15

https://doi.org/10.1016/j.quaint.2020.09.048

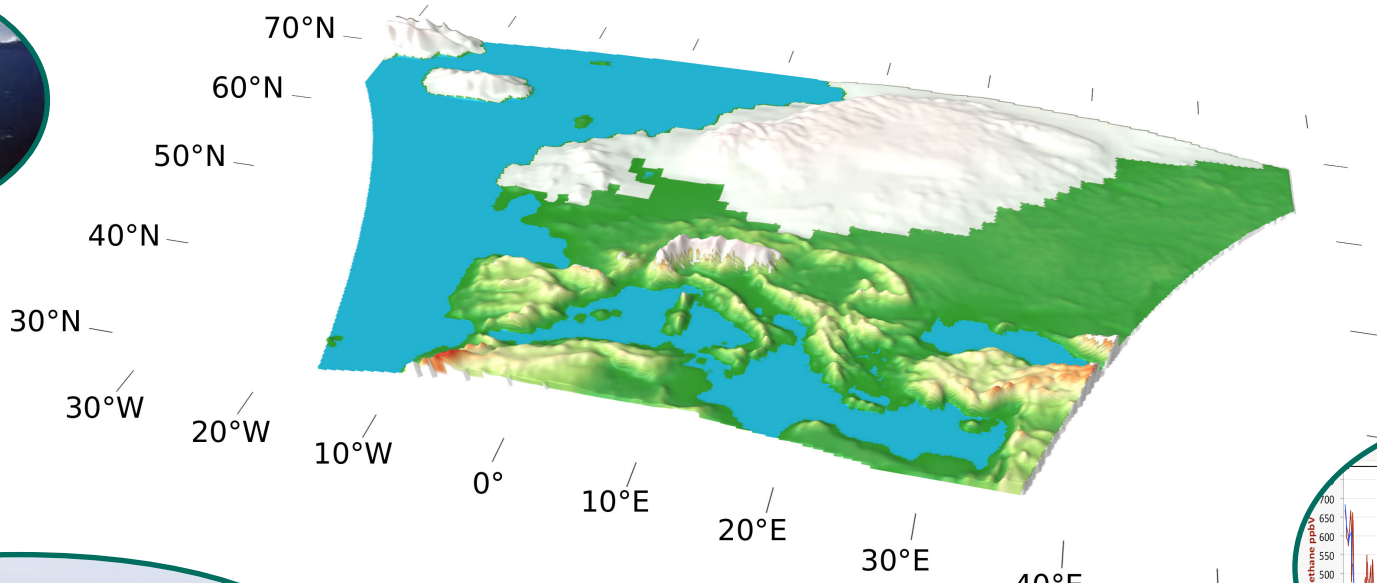
Methods

- Regional climate model simulations with the WRF model (WRF-Chem 4.1.2)
- WRF-Chem includes modules for dust emission, transport and deposition
- Boundary conditions have been adapted to glacial conditions (GHG-concentrations, orbital parameters, land-sea mask, ice sheets, vegetation, …)

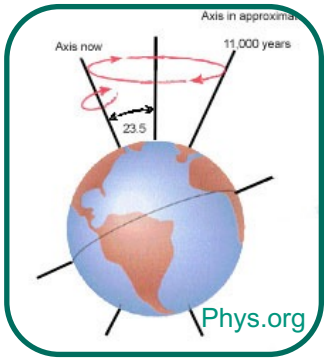


Phys.org

Ice Sheets, Landmask



Ludwig et al. 2019
https://doi.org/10.1111/nyas.13865

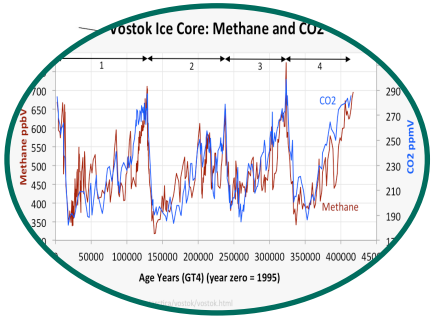


Orbital Parameters

Landuse, Vegetation



geograph.org.uk



Trace Gases

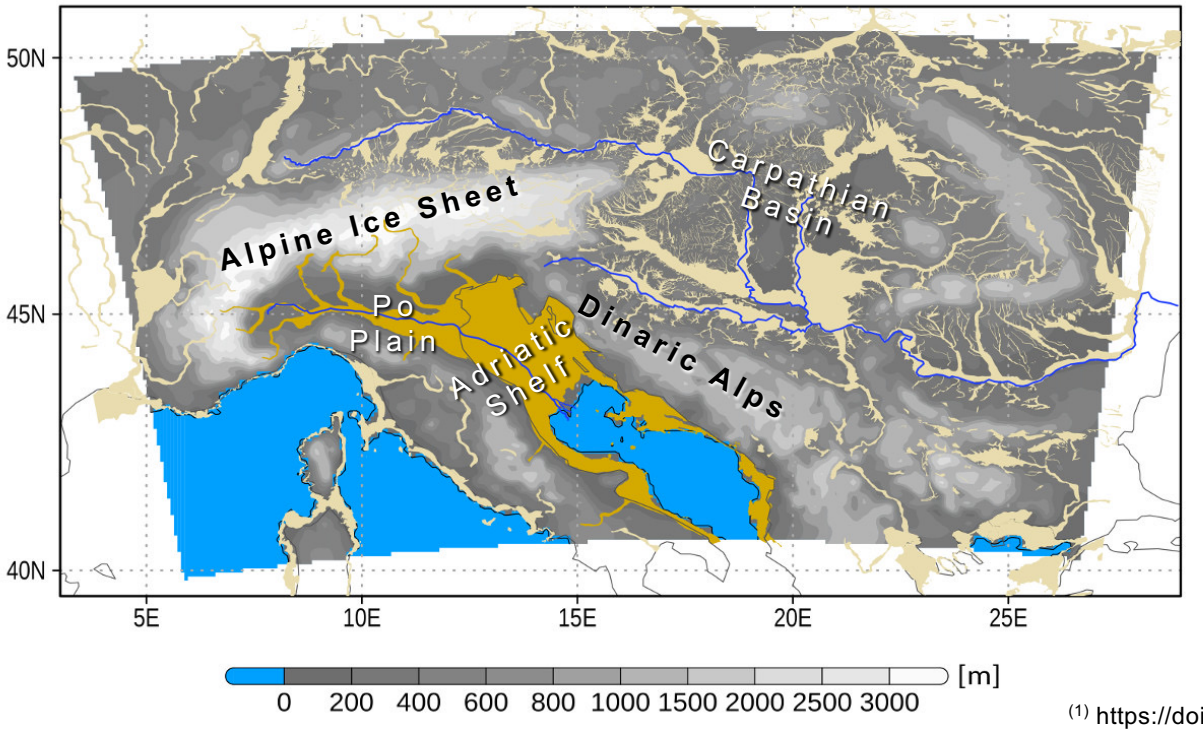
ncdc.noaa.gov

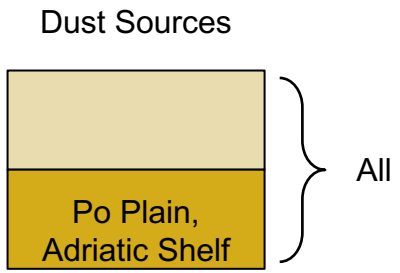
https://doi.org/10.1016/j.quaint.2020.09.048

Methods

- Used data from new loess map (Lehmkuhl[1] et al., 2021) for potential dust sources
- Run WRF model with 8.5 km horizontal grid spacing for 30 years
- Forcing (initial and lateral boundary conditions) from PMIP3 MPI-ESM-P LGM simulation
- Two simulations: (i) all dust sources activated (ii) only dust sources of Po Plain / Adriatic Shelf
- All Figures show 30-year mean values unless otherwise indicated

- Model domain
- Topography
- Dust sources



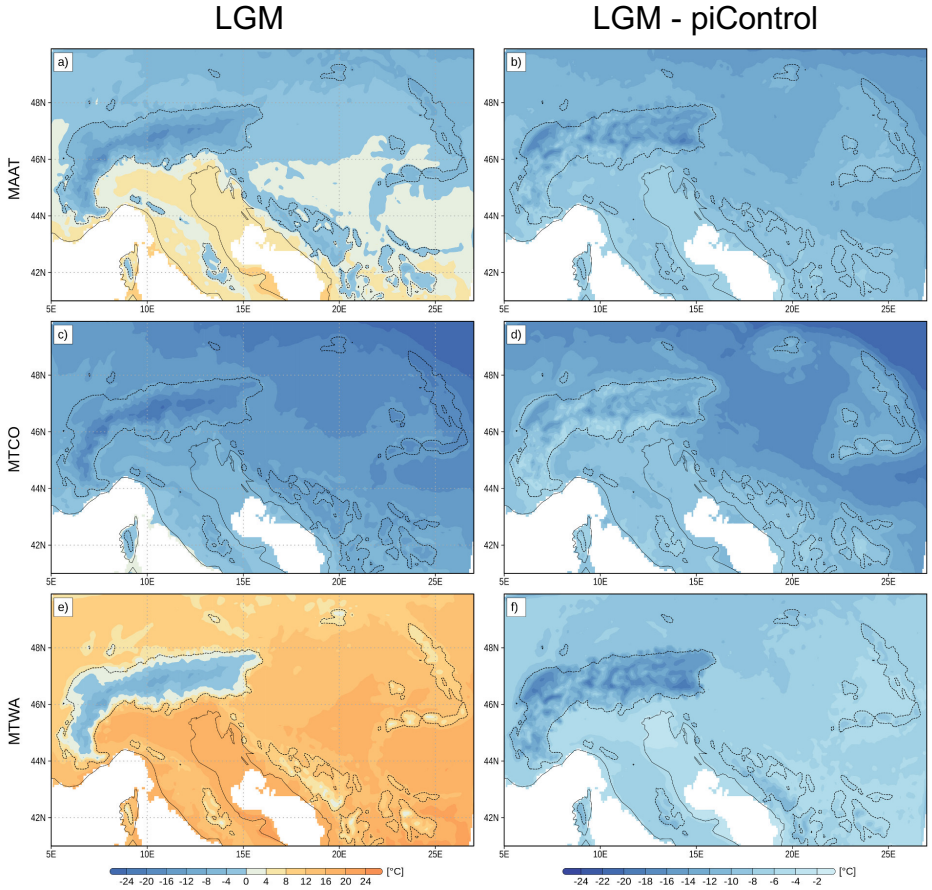


[1] https://doi.org/10.1016/j.earscirev.2020.103496

https://doi.org/10.1016/j.quaint.2020.09.048

Results (Climate)

- Comparison of WRF-LGM and WRF-pre-industrial (pi)Control simulations
- Mean annual air temperature (MAAT), mean temperature of the coldest month (MTCO, January), mean temperature of the warmest month (MTWA, July)



- stronger colling in winter compared to summer
- stronger cooling towards the north (proximity to the ice sheet)
- Comparison with proxy data (Bartlein[1] et al. 2011, BAR):

	MAAT [°C]		MTWA [°C]		MTCO [°C]	
Point [°]	BAR	WRF	BAR	WRF	BAR	WRF
7E; 47N	−11,3 ± 1,69	−12,3	−7,76 ± 1,25	−11,96	−17,95 ± 2,56	−12,0
13E; 41N	−6,6 ± 2,83	−7,4	−7,50 ± 1,71	−7,4	−15,51 ± 3,70	−8,1
15E; 41N	−5,6 ± 2,17	−8,1	−4,18 ± 1,71	−6,9	−14,23 ± 3,62	−8,5
21E; 41N	−5,2 ± 2,19	−8,8	−3,94 ± 1,58	−7,2	−14,19 ± 3,54	−9,1
25E; 41N	−5,1 ± 2,45	−8,6	−7,23 ± 1,53	−4,4	−12,82 ± 3,04	−12,0
27E; 49N	−10,97 ± 1,46	−15,7	−6,07 ± 0,74	−7,7	−17,23 ± 3,15	−20,7
11E; 43N	NODATA	−7,7	−8,04 ± 2,72	−5,9	−17,09 ± 2,37	−9,0

- underestimation of winter cooling, slight overestimation of annual mean cooling

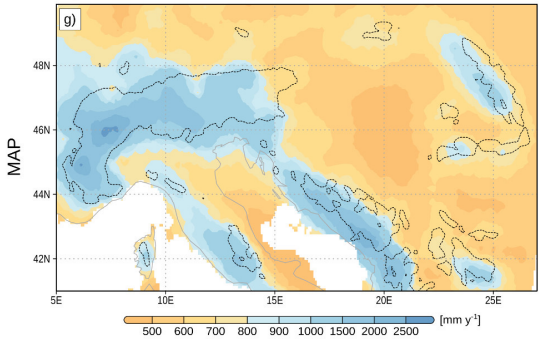
[1] https://doi.org/10.1007/s00382-010-0904-1

https://doi.org/10.1016/j.quaint.2020.09.048

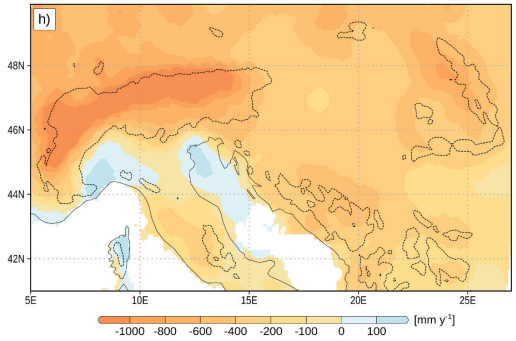
Results (Climate)

- Comparison of WRF-LGM and WRF-piControl simulations
- Mean annual precipitation (MAP)

LGM



LGM - piControl



- much drier conditions during LGM
- Comparison with proxy data (Bartlein[1] et al. 2011, BAR):

	MAP [mm yr^{-1}]	
Point [°]	BAR	WRF
7E; 47N	−440 ± *114*	−931
13E; 41N	−426 ± *99*	−135
15E; 41N	−200 ± *111*	−67
21E; 41N	−240 ± *103*	−245
25E; 41N	−142 ± *64*	−92
27E; 49N	−206 ± *46*	−306
11E; 43N	−369 ± *98*	−149

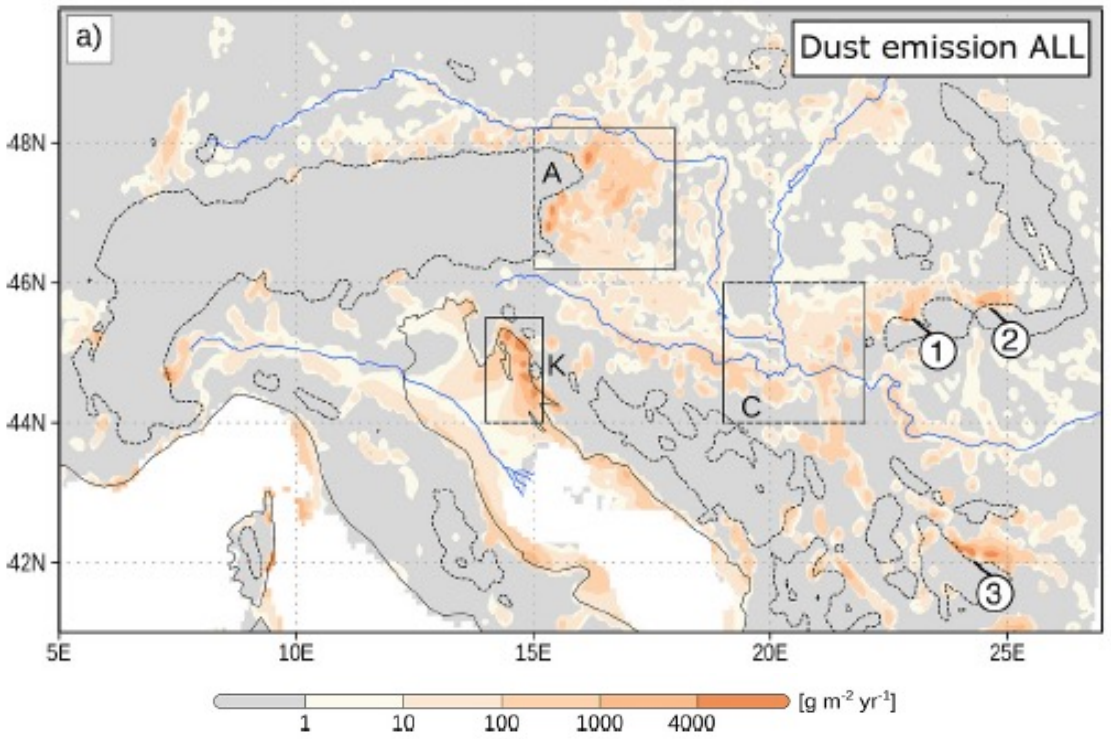
- general good agreement between model and proxy data

[1] https://doi.org/10.1007/s00382-010-0904-1

https://doi.org/10.1016/j.quaint.2020.09.048

Results (Dust)

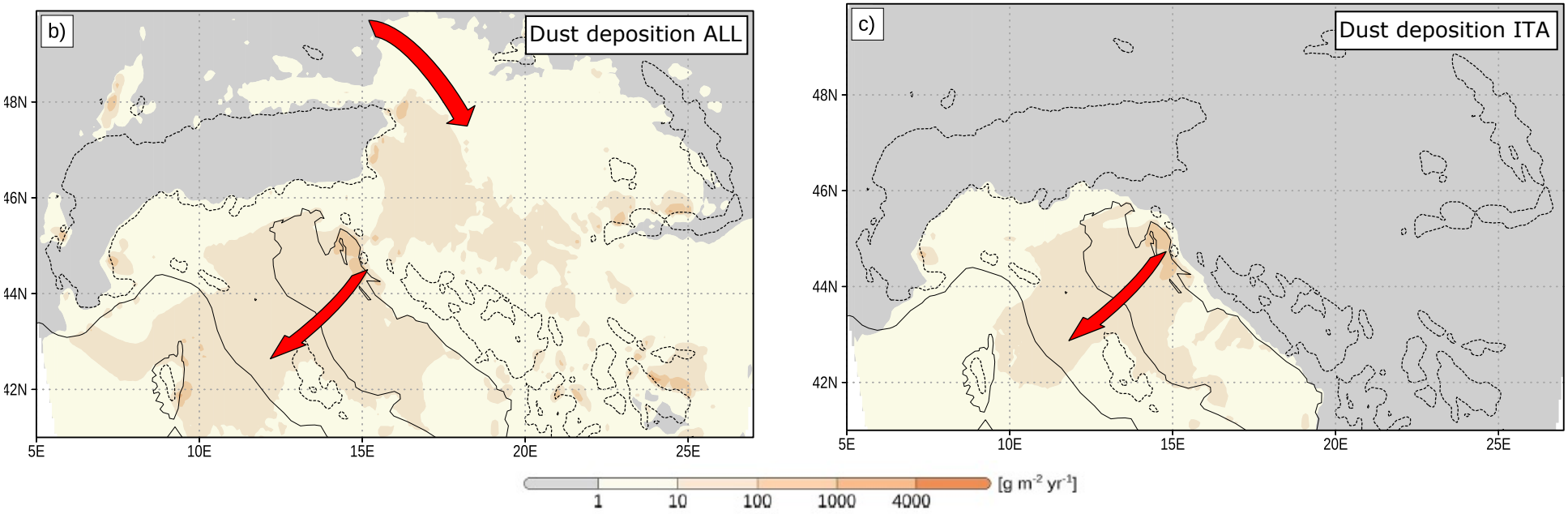
- Dust emission heterogeneously distributed
- Three key areas that will be analysed in more detail
  - (A) Eastern Alps
  - (C) Carpathian Basin
  - (K) Kvarner Bay



https://doi.org/10.1016/j.quaint.2020.09.048

Results (Dust)

- Dust deposition based on all sources and only Po Plain / Adriatic Shelf
- Red arrows represents mean wind direction



- Almost no dust flux between the two basins
- Dinarc Alps act as a natural boundary
- Bora winds responsible for strong dust activity in the Kvarner Bay region?

https://doi.org/10.1016/j.quaint.2020.09.048

Deposition rates

(Carpathian Basin)

Comparison of mass accumulation rates (MAR) and MAR10 (Particles < 10 μm) reconstructed for the LGM period from Loess stacks and simulated deposition rates averaged over the grid box including the stack coordinates and the eight surrounding grid boxes (DEP_{mean}); DEP_{max} denotes the maximum simulated deposition among the nine grid boxes. Simulated deposition rates are limited to grain sizes of up to 20 μm.

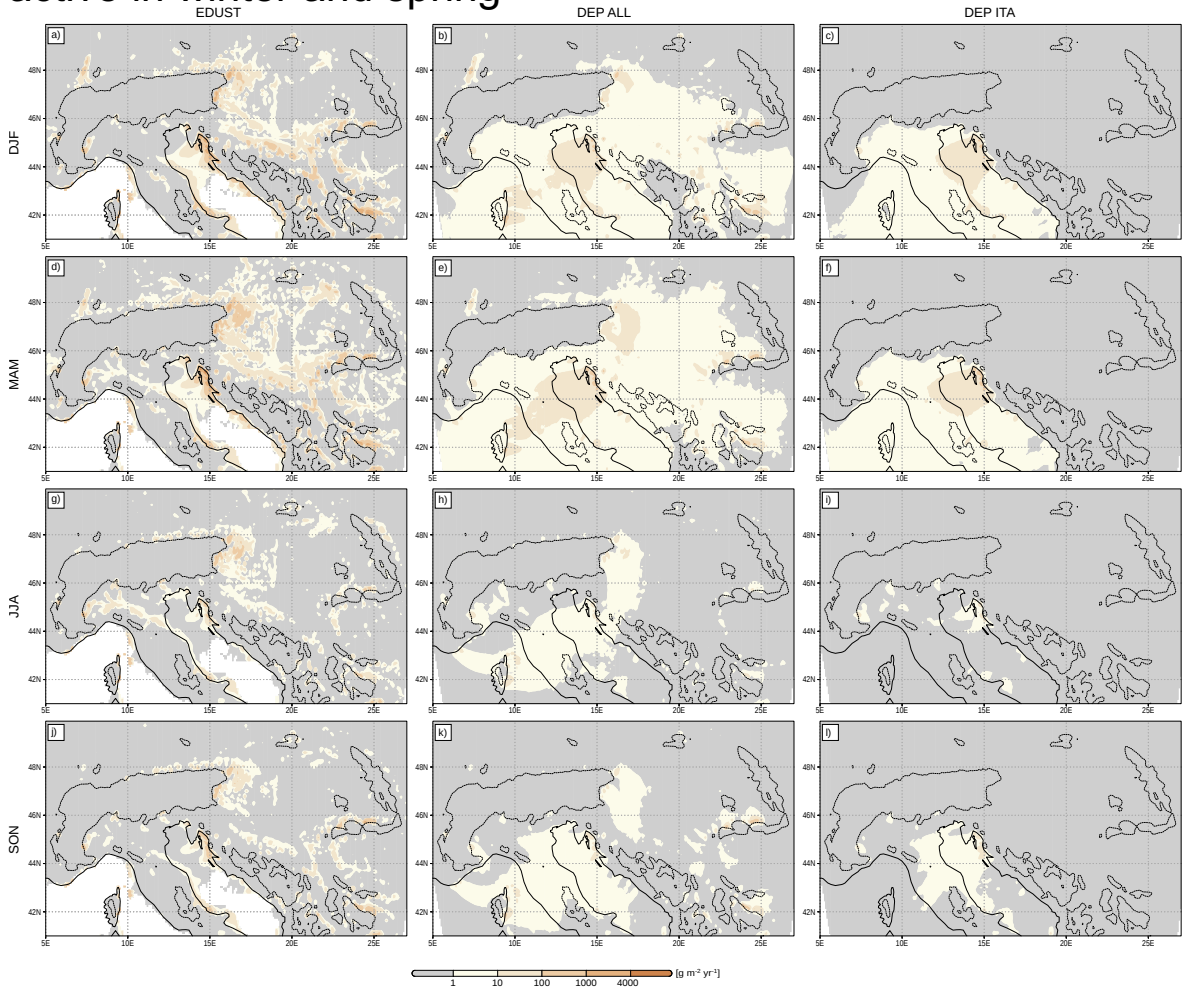
Site	Country	LAT °N	LON °E	MAR g m^{-2} yr^{-1}	MAR10 g m^{-2} yr^{-1}	DEP_{mean} g m^{-2} yr^{-1}	DEP_{max} g m^{-2} yr^{-1}
Albertirsa [Novothny et al., 2002]	HU	47.26	19.64	386.00	96.50	3.60	4.03
Albertirsa [Frechen et al., 2003]	HU	47.26	19.64	841.00	N/A		
Albertirsa [Újvári et al., 2010]	HU	47.26	19.64	587.00	134.00		
Basahare [Újvári et al., 2010]	HU	47.80	18.84	348.00	79.00	2.53	2.96
Batajnica [Újvári et al., 2010]	RS	44.92	20.32	329.00	75.00	15.44	18.65
Crvenka [Újvári et al., 2010]	RS	45.66	19.48	197.00	45.00	10.86	11.78
Debrecen (Alföldi_brickyard) [Újvári et al., 2010]	HU	47.53	21.57	237.00	54.00	3.09	3.29
Dunaújváros [Újvári et al., 2010]	HU	46.97	18.94	1238.00	282.00	5.30	6.50
Erdut [Újvári et al., 2010]	HR	45.53	19.06	215.00	49.00	10.56	11.23
Irig [Újvári et al., 2010]	RS	45.08	19.87	192.00	44.00	10.60	12.83
Katymár [Bokhorst et al., 2011]	HU	46.02	19.20	1005.00	N/A	9.33	9.99
Katymár [Újvári et al., 2010]	HU	46.02	19.20	632.00	144.00		
Lakitelek_I [Újvári et al., 2010]	HU	46.88	20.02	254.00	58.00	5.19	5.73
Látókép [Újvári et al., 2010]	HU	47.56	21.49	212.00	48.00	3.16	3.36
Madaras [Újvári et al., 2010]	HU	46.04	19.29	375.00	86.00	9.10	9.57
Mende [Frechen et al., 1997]	HU	47.42	19.45	456.00	114.00	3.14	3.53
Mende [Frechen et al., 2003]	HU	47.42	19.45	519.00	N/A		
Mende [Újvári et al., 2010]	HU	47.42	19.45	761.00	173.00		
Mosorin [Bokhorst et al., 2011]	RS	45.26	20.28	545.00	N/A	12.82	14.41
Mosorin [Újvári et al., 2010]	RS	45.26	20.28	395.00	90.00		
Paks [Frechen et al., 1997]	HU	46.64	18.88	1325.00	331.25	7.34	8.11
Paks [Frechen et al., 2003]	HU	46.64	18.88	2662.0	N/A		
Paks [Újvári et al., 2010]	HU	46.64	18.88	1422.00	324.00		
Petrovaradin [Újvári et al., 2010]	RS	45.27	19.87	174.00	40.00	13.47	14.63
Ruma [Újvári et al., 2010]	RS	45.01	19.85	192.00	44.00	10.17	11.21
Ságvár [Újvári et al., 2010]	HU	46.83	18.09	176.00	40.00	10.54	11.63
Stari_Slankamen [Újvári et al., 2010]	RS	45.13	20.27	168.00	38.00	15.17	18.65
Surduk [Újvári et al., 2010]	RS	45.07	20.33	434.00	99.00	16.82	19.12
Susek [Újvári et al., 2010]	RS	45.22	19.53	150.00	34.00	13.33	15.73
Süttő [Novothny et al., 2011]	HU	47.74	18.45	1009.0	N/A	2.99	3.61
Süttő [Újvári et al., 2010]	HU	47.74	18.45	584.00	133.00		
Szeged-Öthalom_I [Újvári et al., 2010]	HU	46.28	20.10	332.00	76.00	7.22	7.63
Tápiósüly [Újvári et al., 2010]	HU	47.45	19.52	504.00	115.00	3.05	3.35
Titel [Bokhorst et al., 2011]	RS	45.23	20.30	591.00	N/A	14.41	16.76
Titel [Újvári et al., 2010]	RS	45.23	20.30	510.00	116.00		
Üveghuta-2_borehole [Újvári et al., 2010]	HU	46.20	18.61	338.00	77.00	10.12	11.19
Willendorf_II [Frechen et al., 2003]	AT	47.79	16.05	372.0	N/A	114.97	422.35
Willendorf_II_ [Frechen et al., 2003]	AT	47.79	16.05	886.0	N/A		
Zmajevac [Újvári et al., 2010]	HR	45.81	18.82	437.00	100.00	10.63	11.32

- simulated deposition ~ 15 % of the the MAR10 rates
  - dust transported to the CP from other sources (Sahara, periglacial area of Eurasian ice sheet)
- particles > 20um not considered by the model
  - large particles from local sources (river beds)

https://doi.org/10.1016/j.quaint.2020.09.048

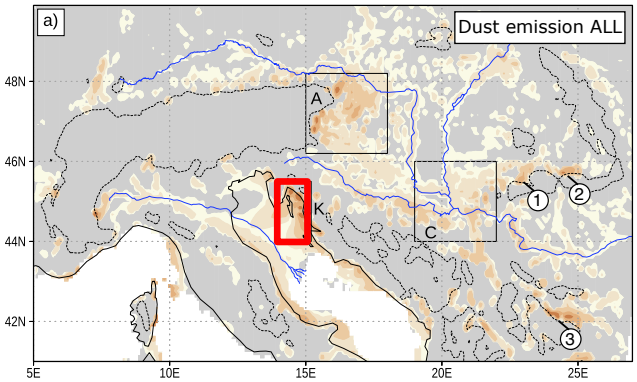
Results (Dust - seasonal cycle)

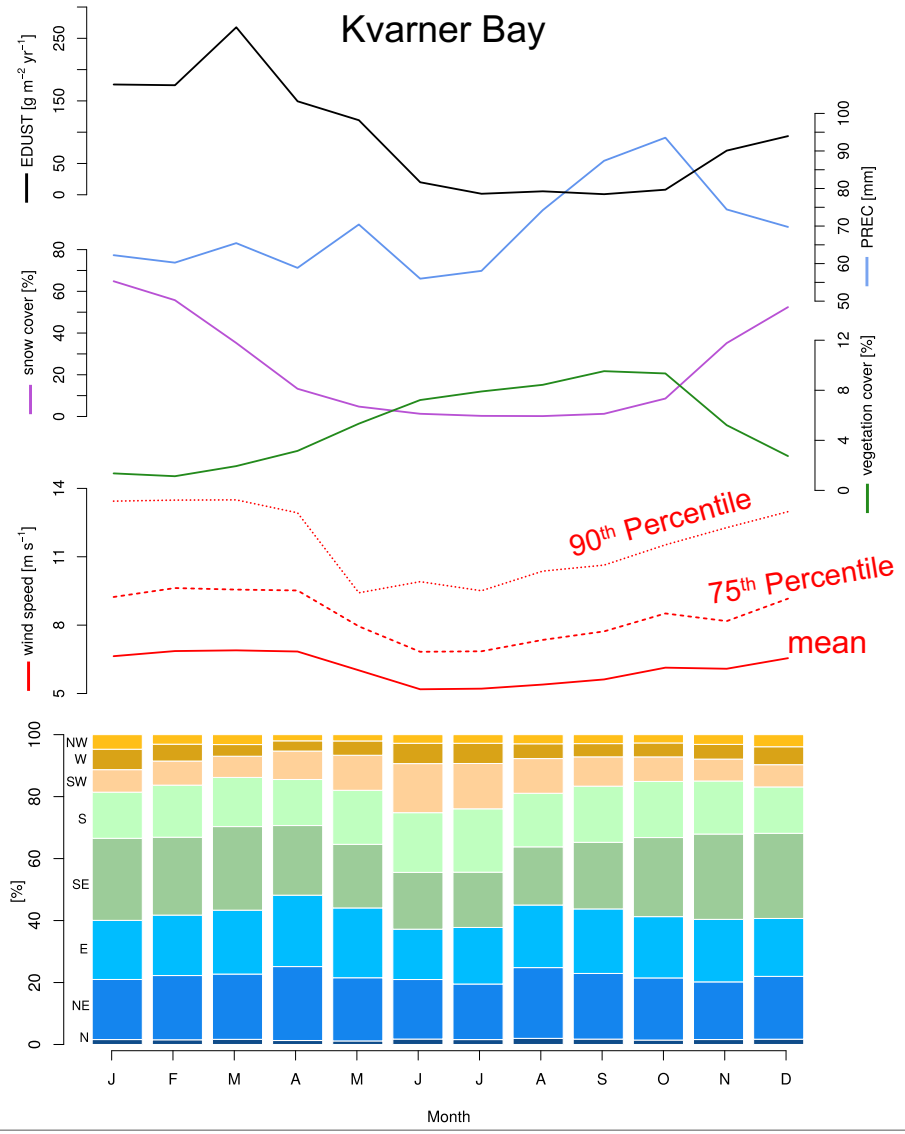
- Seasonal cycle of emission and deposition for all sources and Po Plain / Adriatic Shelf alone
- Dust cycle most active in winter and spring



https://doi.org/10.1016/j.quaint.2020.09.048

Results (Dust emission and Climate)

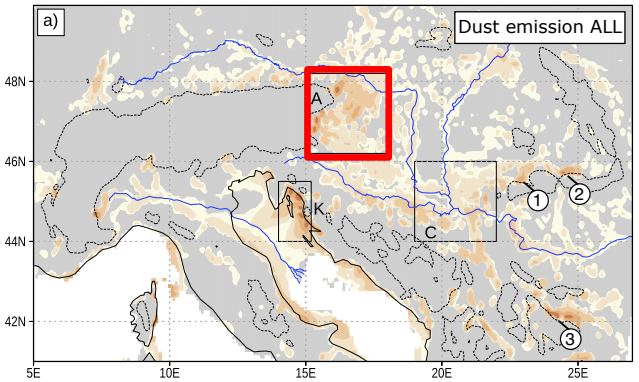


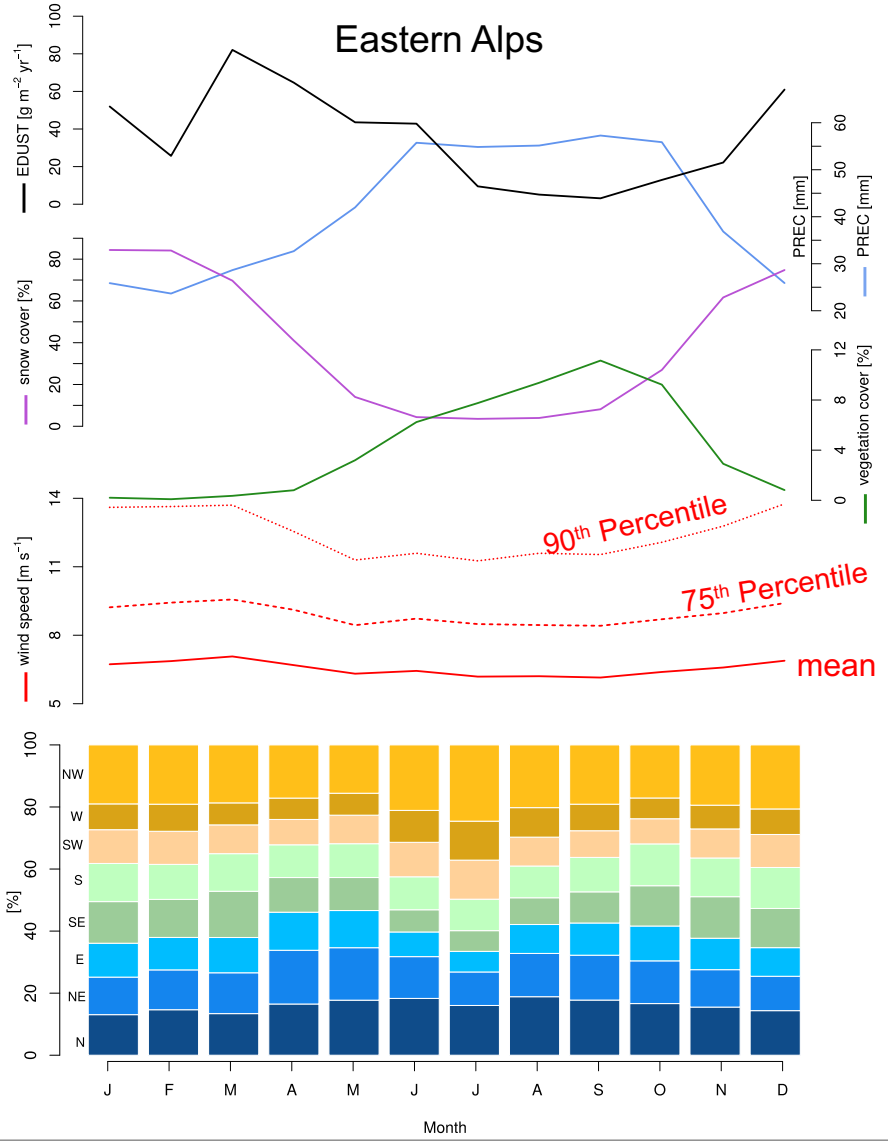


- Peak dust emission late winter / early spring
  - little precipitation
  - strong wind speeds (mean and peak winds)
- Bora winds play key role for dust emission
  - high frequency of easterly winds (NE, E, SE)

https://doi.org/10.1016/j.quaint.2020.09.048

Results (Dust emission and Climate)

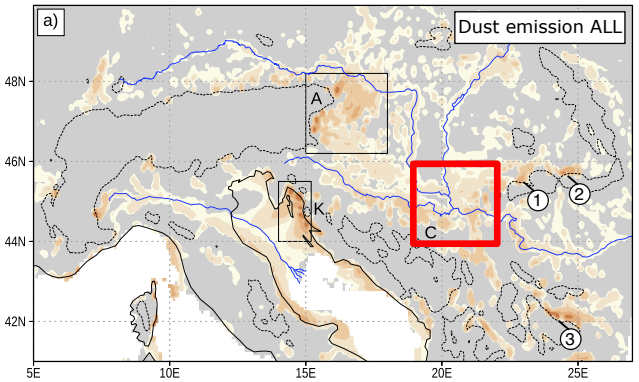


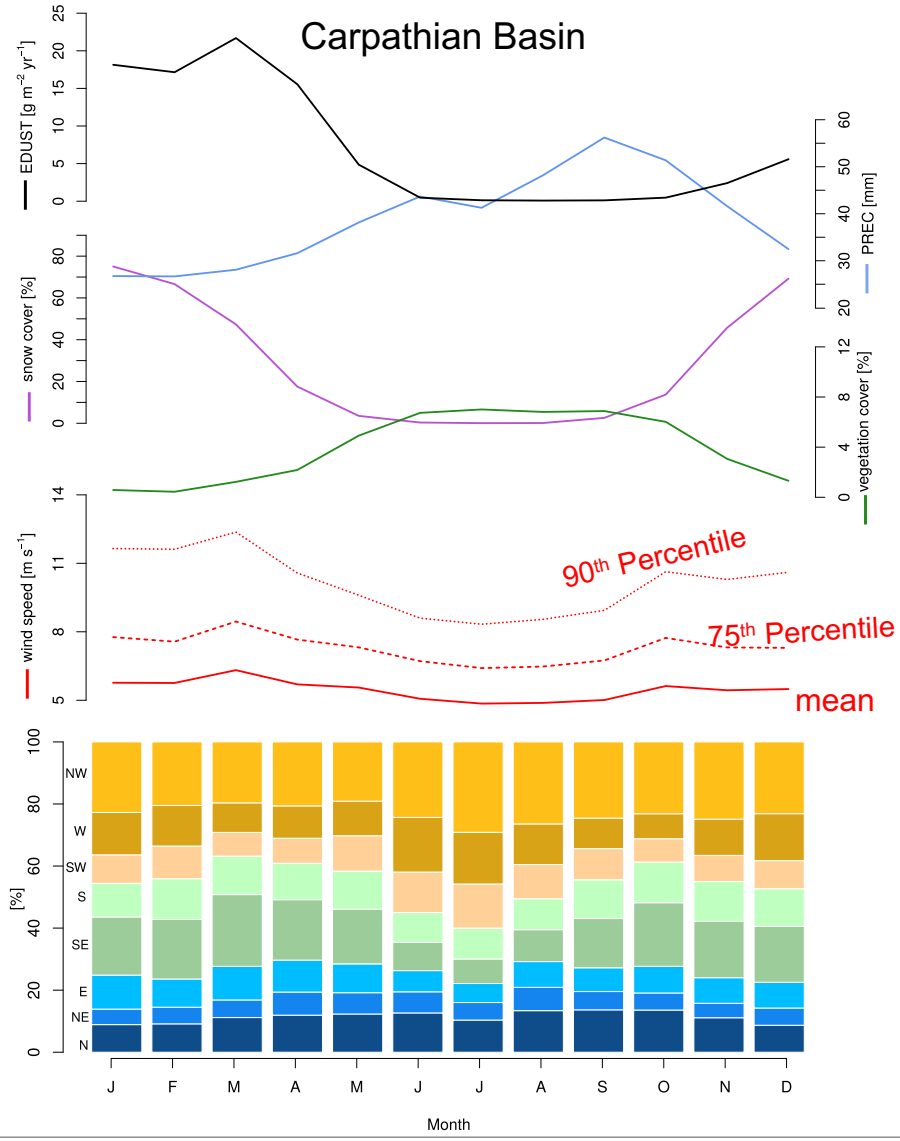


- Peak dust emission late winter / early spring
  - little precipitation
  - strong wind speeds (mean and peak winds)
- Low emissions during summer
  - increased precipitation and vegetation cover
  - reduced wind speeds
- Wind mostly from the north (NE, N, NW)
  - reflected by dune formations (see slide 14)

https://doi.org/10.1016/j.quaint.2020.09.048

Results (Dust emission and Climate)

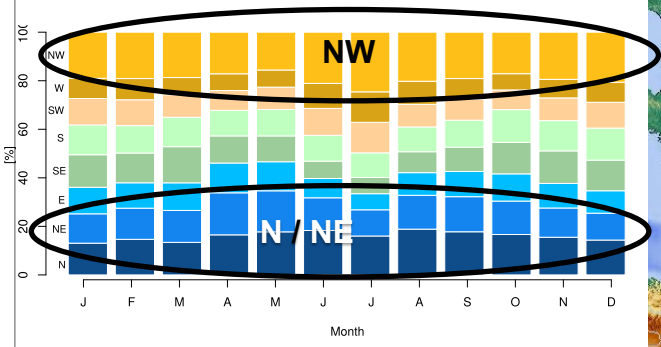


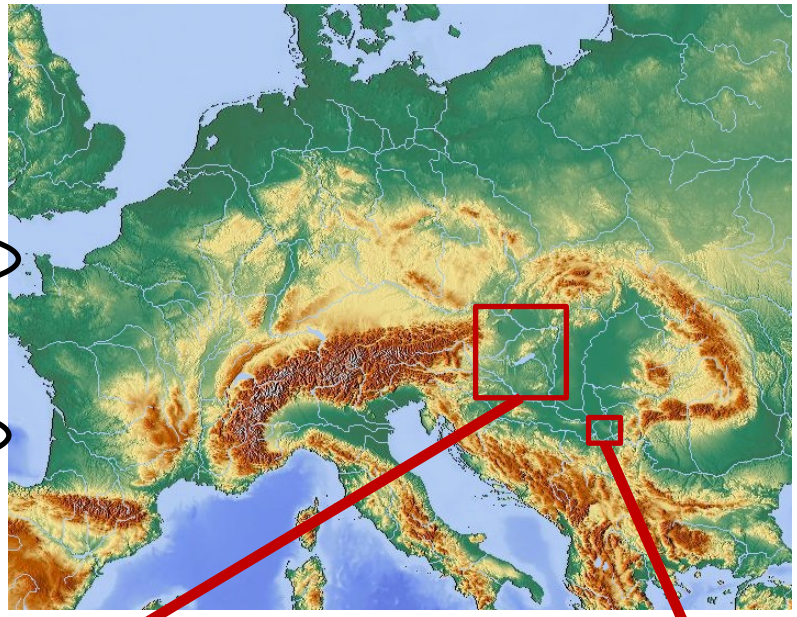


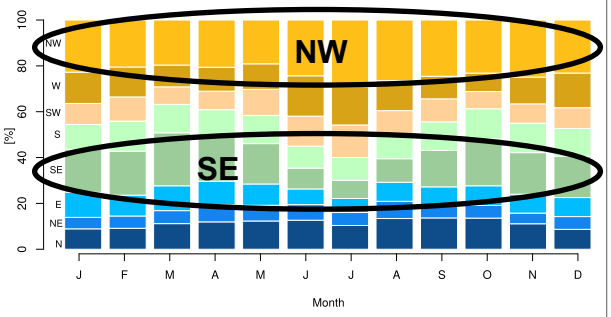
- Peak dust emission late winter / early spring
  - little precipitation
  - strong wind speeds (mean and peak winds)
- Low emissions during summer
  - increased precipitation and vegetation cover
  - reduced wind speeds
- highest wind frequencies from opposing directions (NW and SE) → in agreement with dune formations (see next slide)

https://doi.org/10.1016/j.quaint.2020.09.048

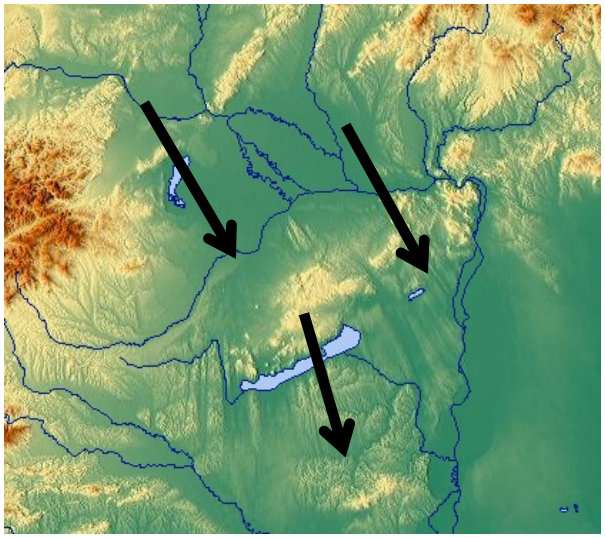
Results (prevailing winds)







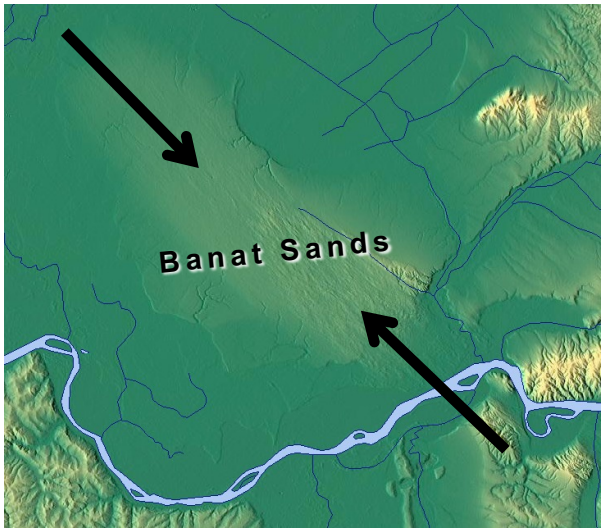
Maps: https://maps-for-free.com/



- Dune orientation in line with prevailing wind directions during LGM

Sebe[1] et al, 2012

Gavrilov[2] et al., 2018



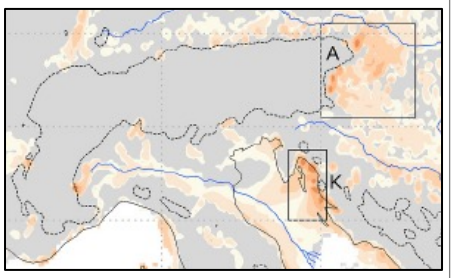
[1] https://doi.org/10.1016/j.geomorph.2011.08.003
[2] https://doi.org/10.1016/j.aeolia.2017.07.008

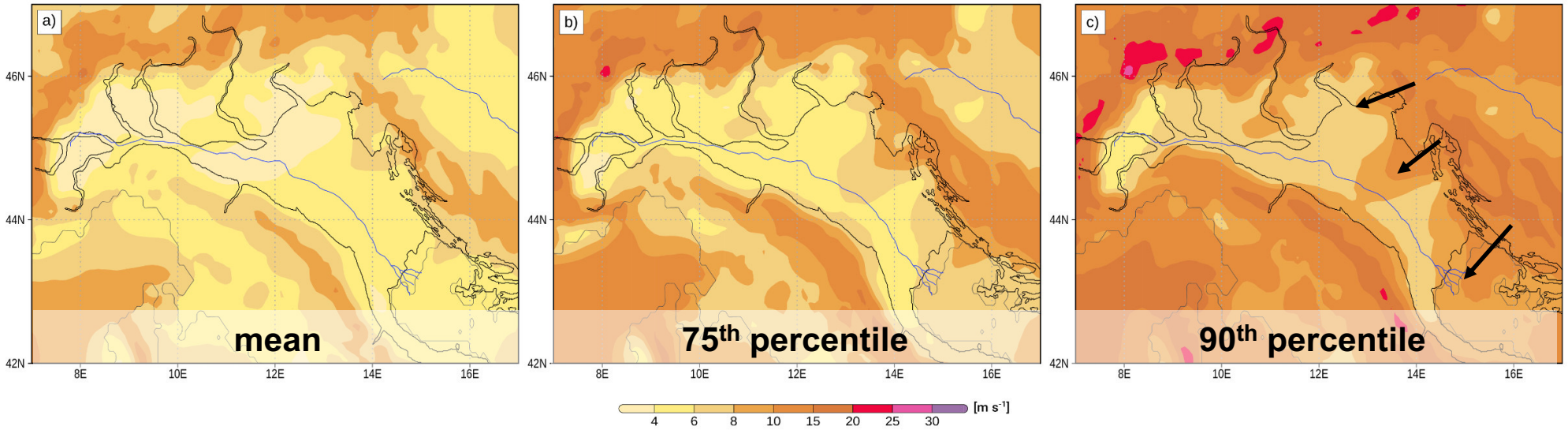
https://doi.org/10.1016/j.quaint.2020.09.048

Results (Adriatic Sea Region)

- Different wind speed characteristics in the Po Plain / Kvarner Bay area
- Wind speeds in Po Plain mostly below threshold for dust emission
  - threshold: ~ 10 - 15 ms^{-1} (e.g. Bullard[(1)] et al., 2016; Cowie[(2)] et al., 2014)
- Stronger wind speeds along the slops of the Dinaric Alps → Bora winds
  - Bora jets (⟶) discernible in the climatology
  - Important role for dust emission in dry fallen Kvarner Bay during the LGM

Dust emission





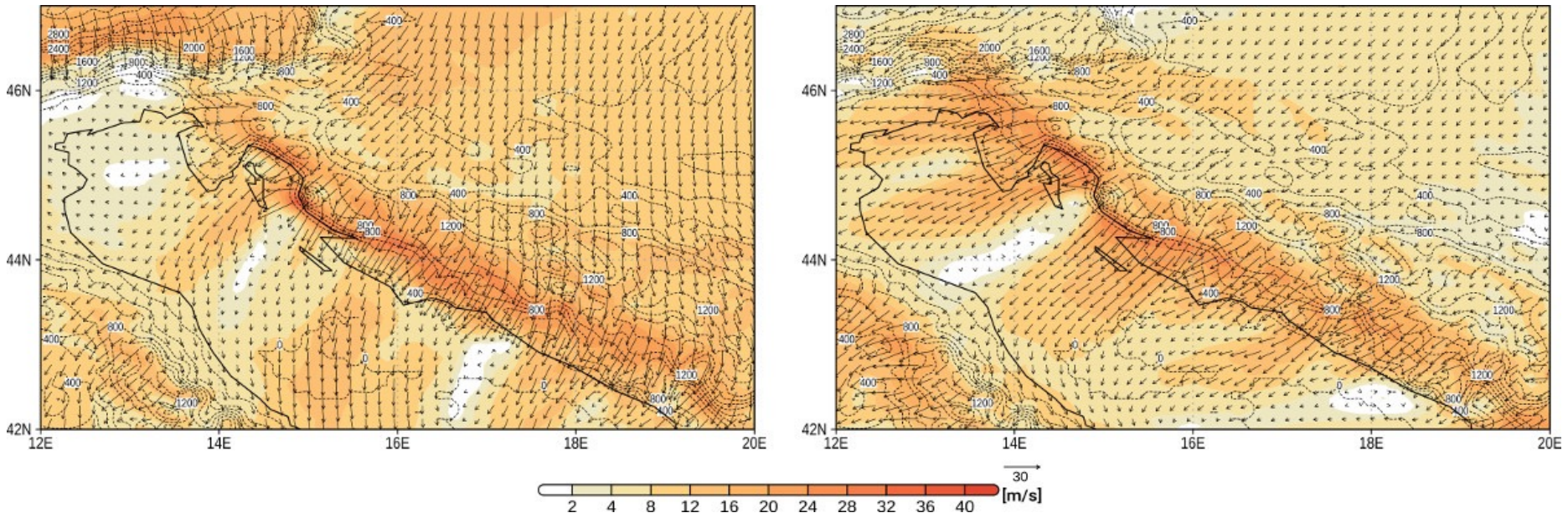
(1) https://doi.org/10.1002/2016RG000518

(2) https://doi.org/10.5194/acp-14-8579-2014

https://doi.org/10.1016/j.quaint.2020.09.048

Results (Bora wind events)

- Daily mean 10-m wind speed (shaded) and wind vectors for two randomly chosen Bora events simulated in March for LGM conditions
- Both simulated bora events show easterly winds inside the domain
- Strong intensification of the flow at the westward slopes of the Dinaric Alps
- This leads to manifestation of typical jet structures



https://doi.org/10.1016/j.quaint.2020.09.048

Karlsruhe Institute of Technology

Results (Dust events alluvial Po Fan)

EGU General Assembly 2021

Event	EDUST [g m^{-2} day^{-1}]	DD	CWT	Wind$_{mean}$ [m s^{-1}]	Wind$_{max}$ [m s^{-1}]
1852-12-15	1048	SW	Cyc	19,05	32,30
1853-03-17	1965	SW	Cyc	16,58	33,80
1854-04-05	2794	SW	Cyc	17,35	32,51
1855-02-26	8320	SW	Cyc	17,67	33,36
1856-08-29	1089	SW	Cyc	16,95	32,39
1857-12-16	1297	SW	W	16,39	27,99
1858-10-24	1209	SW	Cyc	15,99	33,98
1859-04-06	5316	W	W	19,65	34,32
1860-01-24	1371	E	SE	10,78	20,40
1862-04-06	1251	W	Cyc	12,86	31,09
1862-04-08	1444	SW	N	13,70	27,97
1862-12-18	2303	S	Cyc	16,21	28,66
1863-04-18	2169	SW	Cyc	14,63	32,56
1863-08-14	1629	SW	NW	15,18	30,93
1864-01-20	1145	S	SW	14,02	33,70
1869-04-24	2575	SW	Cyc	13,96	29,69
1870-03-10	2033	SW	Cyc	16,27	34,55
1871-03-05	5524	SW	Cyc	16,84	35,56
1872-02-18	10687	SW	W	18,12	37,61
1872-02-19	4669	W	NW	16,03	36,11
1873-05-03	1125	S	SW	11,58	27,84
1876-02-13	2997	S	S	11,21	30,16
1877-03-02	2195	SW	W	16,01	29,36
1877-03-03	1252	SW	Cyc	14,69	30,20
1877-03-06	2290	SW	Cyc	18,38	31,10
1877-03-07	1665	SW	Cyc	12,88	29,80
1878-02-10	1247	SW	Cyc	15,67	28,95
1878-03-17	3343	SW	SW	16,98	33,64
1878-03-22	1277	E	Cyc	11,59	22,17
1879-11-20	1664	SW	S	15,80	34,85
1880-02-22	2314	SW	Cyc	20,23	39,91
1881-02-03	2909	S	SW	13,07	31,45

- Strong dust events also in the alluvial Po fan area (12.0–13.5◦E; 43.5–44,5◦N)
- DD: prevailing wind sector (SW = southwest, S = south, …)
- CWT: synoptic scale circulation pattern (Cyc = Cyclonic)
- Simulated daily mean and max wind speed for each event

➢ Cyclones with strong wind fluctuations additional important component of dust cycle

https://doi.org/10.1016/j.quaint.2020.09.048

Karlsruhe Institute of Technology

Summary

EGU General Assembly 2021

- High resolution regional climate simulation (WRF-model) to study aspects of the regional glacial dust cycle in the Carpathian Basin and Po plain/Adriatic shelf
- High seasonality of the dust cycle (strong during winter/spring, weak during summer/autumn)
- Almost no dust transport between the two regions (Carpathian Basin / Adriatic shelf & Po Plain); Dinaric Alps act as a natural boundary
- Prevailing simulated LGM wind directions in Carpathian Basin in line with dune orientations
- Strong Bora winds responsible for highest dust emission in Kvarner Bay area
- Additionally: cyclonic weather types responsible for sporadic (strong) dust events in alluvial Po fan

Thanks for your interest!

https://doi.org/10.1016/j.quaint.2020.09.048